Progress In Electromagnetics Research, Vol. 145, 185–193, 2014

Thick Metal EBG Cells with Narrow Gaps and Application to the Design of Miniaturized Antennas

Mehdi Hosseini[1, *], David M. Klymyshyn[1, 2], Garth Wells[2], and Xun Liu[1]

Abstract—The paper presents a methodology to achieve efficient low-profile electromagnetic bandgap (EBG) antennas based on thick EBG unit cells. The EBG cells are composed of thick metal patches separated by narrow high aspect ratio (HAR) gaps, and positioned on a PEC-backed substrate. This approach yields new miniaturized EBG cells with considerably reduced electrical size. The miniaturized cells are employed to demonstrate new compact self-excited EBG resonator antennas with considerably reduced operating frequencies. Full-wave simulations and experimental results demonstrate the design approach.

1. INTRODUCTION

The increased demand for miniature wireless systems and sensors has been a motivation for the development of integrated RF front-ends. Although recent advances in fabrication and integration technologies have evolved the way these units are implemented, miniaturization of microwave devices is still a challenge due to fundamental size limitations. In terms of size, most conventional RF components such as filters, power dividers, impedance transformers, and antennas contain structures with feature dimensions of at least $\lambda/4$, or often several times $\lambda/4$. For instance, the well-known branch-line coupler has four $\lambda/4$ sections. The classic patch antenna is $\lambda/2$ long, while its required ground size is typically at least 1.2λ (free-space wavelength) for a satisfactory radiation [1], and reducing its aperture decreases the antenna directivity. Maintaining the radiation efficiency (originating from the ohmic loss) of a small antenna is also a challenge in antenna miniaturization. Consequently, considerable effort has been dedicated to the design of efficient and compact passive RF components [1–10]. A number of size reduction methods have been studied, including using fractal-shaped patterns [10], applying dielectric [2] or magnetic [11] materials around the element, utilizing lumped [2] or parasitic [1] elements, applying metamaterial based ideas [9], enhancing the slow-wave behavior through periodic loading [12], etc..

The electromagnetic bandgap (EBG) concept [3–7] has also demonstrated remarkable potential for size reduction and various other advantages such as bandwidth and gain enhancement, surface wave suppression, and loss mitigation. More specifically, it has been repeatedly shown that incorporating EBG cells into RF structures can reduce their resonance frequency (f_r) [6–7, 13]. One salient advantage of EBG structures is that they can be used along with substrates with high relative permittivities (ε_r) [14] to yield a lower resonance for RF devices such as antennas, while still suppressing surface waves.

This work focuses on new thick metal EBG cells and discusses cell miniaturization and its applications to antenna size reduction. Miniaturization techniques to reduce the resonance frequency of the basic unit cell using a Bloch-based cell modeling approach are presented. Improved, compact EBG cells are applied to the structure of a new-type of antenna called self-excited EBG resonator antenna (SE-EBG-RA), first presented in [5]. The original SE-EBG-RA with the basic EBG cell [5] is compared

Received 15 February 2014, Accepted 10 March 2014, Scheduled 24 March 2014

* Corresponding author: Mehdi Hosseini (m.hosseini@usask.ca).

[1] Department of Electrical and Comp. Eng., University of Saskatchewan, Saskatoon, SK, Canada. [2] Synchrotron Laboratory for Micro and Nano Devices, Canadian Light Source, Saskatoon, SK, Canada.

to the new version developed here with improved cells. An antenna prototype using one of the proposed unit cells is designed and fabricated. The experimental results for the prototype validate the theoretical and numerical modeling proposed in the paper.

2. EBG CELL DEVELOPMENT AND MINIATURIZATION

The progression towards a miniaturized thick-metal EBG unit cell is shown in Fig. 1. The basic cell in Fig. 1(a) can be considered a type of via-less version [3] of the mushroom-like cell [7, 15], composed of electrically small thin metal patches on top of a PEC-backed dielectric substrate. The idea to attain new cells is to thicken the top metal layer considerably, while manipulating the lateral metal pattern to reduce the cell resonance frequency. The ensuing EBG structures proposed in this study (the antennas in Section 3) comprise a number of these thick patches deployed periodically in one dimension (1D EBG structure), and with very tiny gaps between cells. The gaps typically have very high aspect ratios (HAR) (Fig. 1(b) example has AR = 2 mm/0.1 mm = 20), and therefore introduce a high capacitive coupling effect that significantly reduces the cell electrical size.

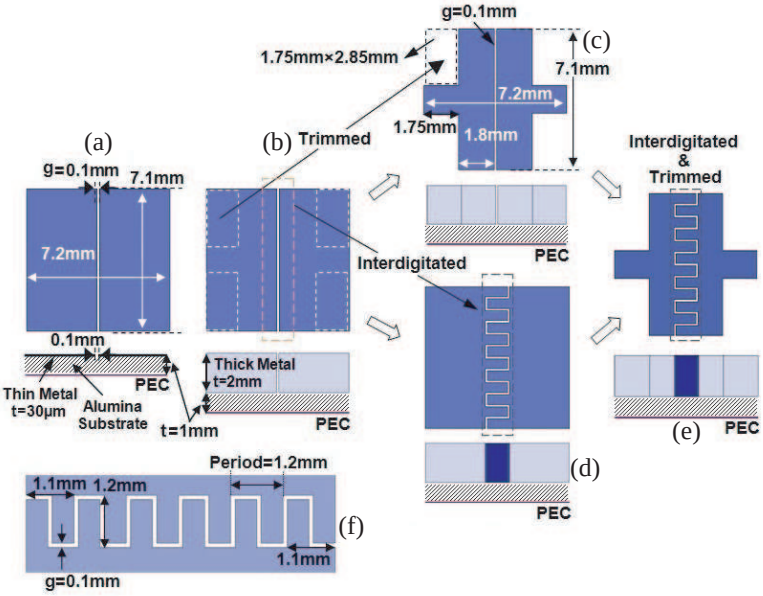

Figure 1. Step-by-step development and miniaturization of the thick metal EBG unit cell (side/top views depicted); the substrate in this example is alumina with $\varepsilon_r = 9.9$ and $\tan\delta = 0.003$; the aspect ratio, AR, is t/g.

2.1. Thickening, Interdigitation, and Trimming

There are a number of methods proposed to tailor the properties of EBG cells such as interdigitation [6, 16, 17], trimming [9], and much less commonly, thickening [5, 18, 19]. In this section, these methods are applied to the thin via-less mushroom-like EBG cell in Fig. 1(a), both separately and in combination, with the objective to develop a new type of EBG cell with dramatically reduced electrical size.

First, the thickness of the metal layer of the thin EBG cell in Fig. 1(a) is increased considerably, in this example to 2 mm while the gap remains constant at 0.1 mm. This turns the cell into a very thick EBG cell with a HAR gap (AR = 20), as shown in Fig. 1(b). Fig. 2 and Table 1 compare the cell properties in the progression from cell 1(a) to 1(b), showing that the cut-off frequency (f_c) decreases from 4.83 GHz to 3.43 GHz (29% drop). Fig. 2(b) shows the cell dispersion diagram generated by the HFSS/Bloch method described in [5]. The method renders two curves for each cell, which are the

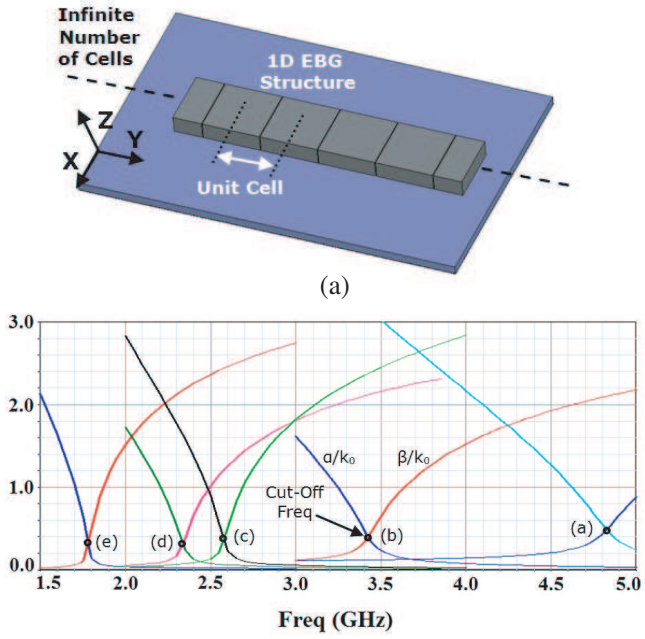

Figure 2. (a) 1D array structure of the EBG cell in Fig. 1(b); (b) complex propagation constant ($\gamma = \alpha + j\beta$) along Y-axis normalized by free-space wavenumber (k_0) for EBG cells described in Fig. 1/Table 1. The twin curves (a) to (e) are related to Figs. 1(a) to (e) and Result 1 to 5 in Table 1.

Table 1. Electrical and physical properties of the EBG cells in Fig. 1; λ_c is the wavelength at f_c.

	Thin EBG	**Thick/Tall EBG**			
	Result 1 Fig. 1(a)	**Result 2 Fig. 1(b)**	**Result 3 Fig. 1(c)**	**Result 4 Fig. 1(d)**	**Result 5 Fig. 1(e)**
Cut-off Freq (GHz)	4.83	3.43	2.58	2.34	1.78
Cell Size (mm)	7.2 (λ_c/8.6)	7.2 (λ_c/12.15)	7.2 (λ_c/16.15)	7.2 (λ_c/17.8)	7.2 (λ_c/23.5)
Overall Thickness (mm)	1 (λ_c/62)	3 (λ_c/29.2)	3 (λ_c/38.8)	3 (λ_c/42.7)	3 (λ_c/56)
Cell Size Shrinkage (times)	1	1.41	1.87	2.06	2.7
Footprint Shrinkage (times)	1	2	3.5	4.25	7.3

real (α) and imaginary part (β) of the complex propagation constant (γ) along a 1D array (in the Y direction shown in Fig. 2(a)) made of an infinite number of cells. In this method, the array in Fig. 2(a) is considered a transmission line (TL), composed of EBG cells (EBG TL). The f_c reported in Table 1 is where these two curves intersect as highlighted in Fig. 2(b).

The next method applied is to trim some rectangular pieces of the thick metal layer shown in Fig. 1(b), to obtain the cell in Fig. 1(c). This modification turns the cell into a 1D dogbone-like cell, the 2D version of which is known as Jerusalem cross cell [20]. As in Table 1 and Fig. 2, this change decreases f_c again, from 3.43 GHz to 2.58 GHz (25% drop). The next attempt is to apply interdigitation rather than trimming. To do this, the cell in Fig. 1(b) is considered and its HAR gap is interdigitated towards increasing the gap capacitance, as shown in Fig. 1(d). The details of the example interdigitation are given in Fig. 1(f). As seen in Fig. 2 and Table 1, this reduces f_c from 3.43 GHz to 2.34 GHz (32% drop).

2.2. HAR Interdigitated Dogbone EBG Cell

The next step after separately demonstrating the miniaturization effects rendered by trimming and interdigitation is to combine and simultaneously apply them to the cell in Fig. 1(b). Fig. 1(e) shows what the ensuing cell resembles and that this combination reduces f_c from 3.43 GHz for Fig. 1(b), to 1.78 GHz for Fig. 1(e) (48% drop). Table 1 compares the electrical and physical properties of all five EBG cells depicted in Fig. 1. The results clearly demonstrate a gradual and remarkable reduction in f_c of the cells. It is worth noting that by switching from Result 1 (f_c = 4.83 GHz) to Result 5 (f_c = 1.78 GHz), f_c dramatically drops by 63%, i.e., 2.7 times lower. Since the cell is spread two dimensionally, this is approximately equal to the shrinkage achieved in both the X and Y directions of the 1D array, resulting in an array footprint which is 7.3 (2.7^2) times smaller, in terms of the new λ_c (at the new f_c). It is worthwhile to note that starting from the cell in Fig. 1(a) and ending with the cell in Fig. 1(e), the lateral physical dimensions and the substrate material are unchanged, and the only modification is to increase the metal layer thickness and manipulate the lateral pattern.

2.3. Physical Comparison of Presented Cells

To show the actual size reduction potential, the cells in Figs. 1(b) and (e) are scaled down in size, and designed to operate at the same f_c as the basic cell (Fig. 1(a)), all with the same substrate permittivity. Therefore, all cells shown in Fig. 3 resonate at 4.83 GHz (identical λ_c), however their physical dimensions are considerably different, and easy to compare visually.

As shown in Fig. 3, the overall thickness of the last cell, i.e., from the PEC ground to the top of the metal layer, is only 1.1 times larger (h increases to 1.1 h in Fig. 3) than the first (roughly the same) while its cell size is 2.7 times smaller than the first cell. It is worth noting that the footprint is noticeably smaller as it is reduced two dimensionally (by 2.7^2 or 7.3 times). This means that the application of interdigitation and trimming causes the ensuing cell to only occupy 13.7% of the surface area taken by the basic thin EBG cell (with identical f_c).

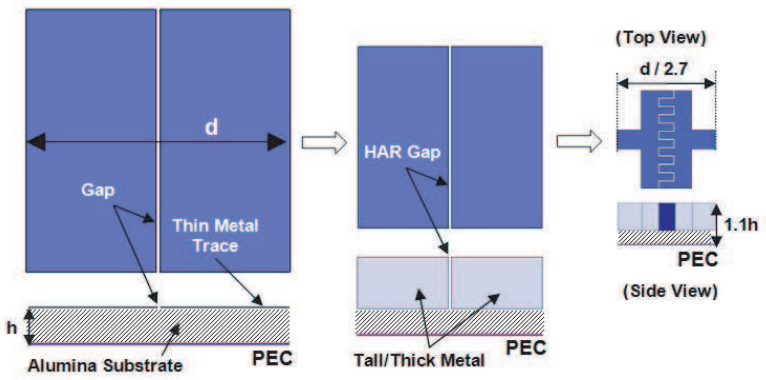

Figure 3. Visual comparison between the size, thickness, and footprint of the EBG cells in Table 1. Dimensions of EBG cells (b) and (e) in Fig. 1 are scaled to operate at the same resonance frequency (f_c = 4.83 GHz) of the basic thin EBG cell (a).

2.4. The Advantage of Thick Interdigitated Gaps

When creating an interdigitated capacitor with gaps in thin metal layer (Fig. 1(a)), the couplings between interdigits are largely coplanar, occurring outside the gap. This practically limits the number of possible interdigitated arms because more interdigits reduces the width of each, and lowers the coplanar coupling. In contrast, with HAR gaps (Figs. 1(d) and (e)), the dominant coupling mechanism is parallel plate capacitance. In this case, gap capacitance is relatively high, electric fields are contained mainly within the HAR gaps, and the number of interdigits can be increased considerably, up to minimum feature size and maximum AR limitations of the fabrication process. Deep X-ray lithography with metal electroforming, for instance, has been used to realize ARs of > 50 for metal microwave

devices [8], and with very smooth side walls. Such HAR microfabrication methods allow the designer to reach considerable degrees of freedom to trade-off the number and length of interdigits with metal thickness to drastically reduce the cell size and the size of antennas incorporating these cells, while at the same time improving other antenna characteristics such as radiation efficiency. In addition, the via-less nature of the proposed thick metal cells can considerably simplify the fabrication process.

3. APPLICATION OF MINIATURIZED EBG CELLS TO ANTENNA DESIGN

This section demonstrates the potential for miniaturizing antennas using the proposed cells, by applying them to a novel antenna concept first presented in [5], the self-excited EBG resonator antenna (SE-EBG-RA). The SE-EBG-RA in this case is made of three cascaded thick metal EBG unit cells (cell size $\ll \lambda_r$, at the matching frequency, f_r) forming an open circuit microstrip-fed EBG TL. The antenna configurations for two types of cells are shown in Figs. 5 (a) and (b). The SE-EBG-RA input impedance can be found from [5]:

$$Z_{in} = Z_B / \tanh \gamma l \tag{1}$$

where Z_B, the Bloch line impedance, and γ of the EBG TL (both along Y-axis in Fig. 2(a)) can be found using the HFSS/Bloch method [5]. Here l is the total antenna length, which in case of the 3-cell antenna structures considered here is 3 times the cell size ($l = 3 \times 7.2$ mm for all cells). Using (1), dB$|S_{11}|$ of different versions of SE-EBG-RA with cells shown in Figs. 1(c), 1(d), and 1(e) are calculated and compared in Fig. 4. The results show a gradual reduction in f_r. As expected, this behavior corresponds to the gradual decrease in $f_c (f_c \neq f_r)$ already observed in Fig. 2(b) and Table 1.

For comparison, two of four cases in Fig. 4 are modeled in HFSS and analyzed completely numerically. This provides independent results that can be compared with the result in Fig. 4 obtained by HFSS/Bloch method. The antennas in Figs. 5(a), and 5(b) with identical substrate and physical size are compared, and the radiation patterns are depicted in Figs. 5(c) and 5(d), respectively (realized gains). The related dB$|S_{11}|$ and efficiency are also compared in Fig. 6. As observed, f_r in both cases agrees very well with the results shown in Fig. 4.

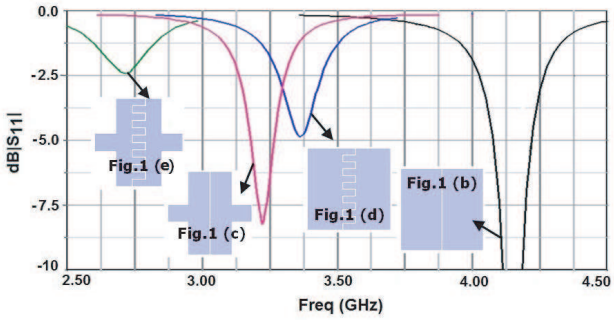

Figure 4. Comparison of the input matching of SE-EBG-RAs composed of different EBG cells in Fig. 1; results are based on HFSS/Bloch method [5].

Although the antennas in Fig. 4 do not target any specific frequency band and are only rendered for demonstration, as observed, they are operating close to some popular bands like unlicensed ISM 2.4 GHz [21] or WLAN (2.4/5 GHz). Therefore, in case a designer is interested in such miniaturized designs, it is possible to use either scaling or a computationally affordable fine-tuning approach to adjust f_r to the desired frequency. Specifically indicating the left cell in Fig. 4, it is observed that the 3-cell SE-EBG-RA based on the cell is matched at 2.7 GHz which is very close to 2.4 GHz ISM band. It should also be noted that when using different cells in Fig. 4, to keep comparisons easy and reasonable, the antenna feedline has not changed (at the same size used for the cell on the right, to have 50 Ω). This condition causes the other three antennas to resonate (the reactive part of Z_{in} crosses zero), but not exactly be matched to 50 Ω. A $\lambda/4$ transformer can then be designed and added to each antenna to match them to 50 Ω. Due to the high permittivity of the substrate ($\varepsilon_r = 9.9$), the physical length added by the transformer will be very small.

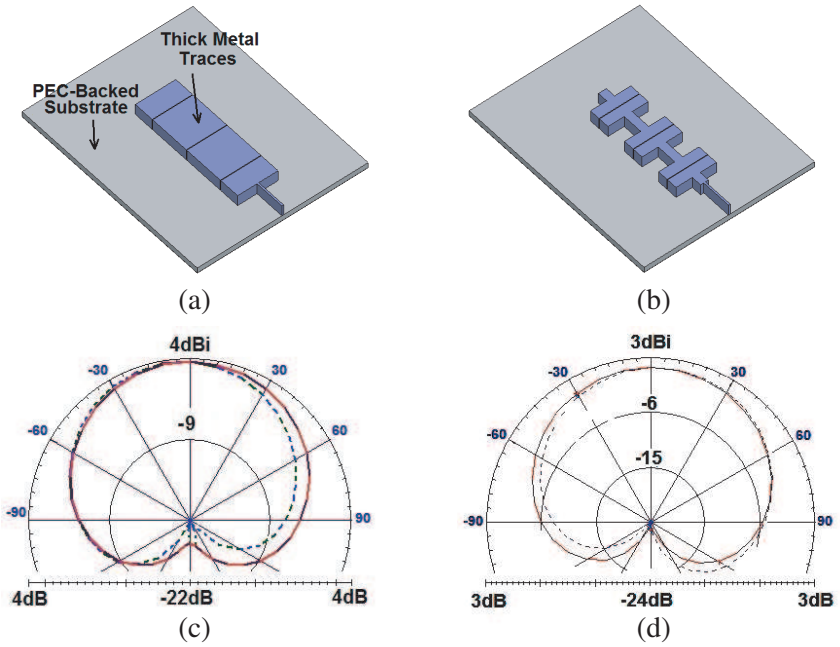

Figure 5. 3D view of SE-EBG-RAs composed of EBG cells in Figs. 1(b) and (c); Radiation pattern (c)/(d) corresponds to the antennas in (a)/(b); Dashed/solid line is the E/H-plane pattern; ground plane size is 30×37 mm; input 50 Ω MSLs are 0.3 mm wide, 5.25 mm long, and 2 mm tall (the same as cells); cells dimensions are provided in Fig. 1.

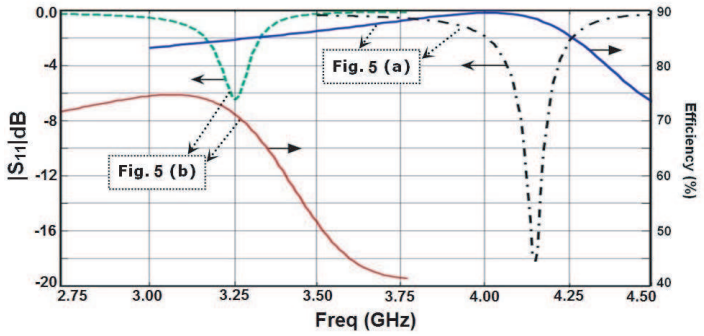

Figure 6. Comparison of the matching frequency and efficiency for the SE-EBG-RAs in Fig. 5; based on full-wave analysis.

Table 2. Dimensions and characteristics of the prototype unit cell; physical parameters are defined in Fig. 1. Δ is the difference between HFSS and HFSS/Bloch results divided by the HFSS/Bloch result.

$\varepsilon_r = 10.2$, $\tan\delta = 0.002$ (Rogers RO3010), $w = 7.1$, $d = 7.3$, $t = 10$, $g = 0.6$ (AR = 16.6), and $h = 1.27$ (all in millimeter)				
	Experiment	HFSS/Bloch	HFSS	Δ
Overall Thickness $(h + t)$	$11.27(\lambda_r/6.54)$			
Cell Size (d)	$7.3(\lambda_r/10.1)$			
Matching Freq, f_r (GHz)	3.98	3.95	4.07	3%

4. EXPERIMENTAL VERIFICATION

In this section, a sample unit cell is considered in Table 2, and an antenna prototype based on this cell is fabricated and measured to verify the approach. In this case, the cell described in Table 2 has a relatively large gap (0.6 mm) and high AR of 16.66 (10 mm/0.6 mm), and is suitable for fabrication with CNC-milling for demonstration purposes. Much smaller gaps and structures could be realized with deep X-ray lithography, or other suitable HAR microfabrication techniques.

As shown in Fig. 7, the machined parts are glued on a copper backed Rogers RO3010 substrate. The 0.6 mm gaps are realized by inserting plastic shims between adjacent parts and then removing them after the glue is hardened. A thick metal microstripline between the SMA connector and the first cell acts as a quarter-wave impedance transformer to match the input to 50 Ω. Fig. 7 compares dB$|S_{11}|$ for both fabricated and simulated versions. As seen, the dB$|S_{11}|$ results are in a very good agreement, providing confidence in the simulations and numerical analyses presented in the paper. For this antenna, the efficiency calculated by HFSS at resonance (4.07 GHz) is 94%. Measurements using the Wheeler cap method [22] give an efficiency of ∼87% (see Fig. 8) with ±5% uncertainty observed when repeating the measurement. Fig. 8 shows the cap mounted onto the antenna shown in Fig. 7, with a ground plane size of $0.49\lambda_r \times 0.39\lambda_r$. The simulated gain and front-to-back ratio for this ground plane size are 3.9 dBi (in broadside direction) and 8.75 dB, respectively.

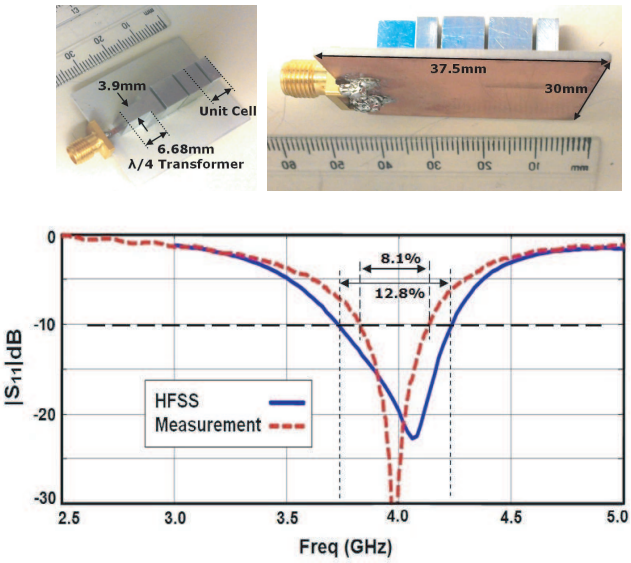

Figure 7. The fabricated SE-EBG-RA together with its measured and simulated dB$|S_{11}|$; bandwidths are highlighted.

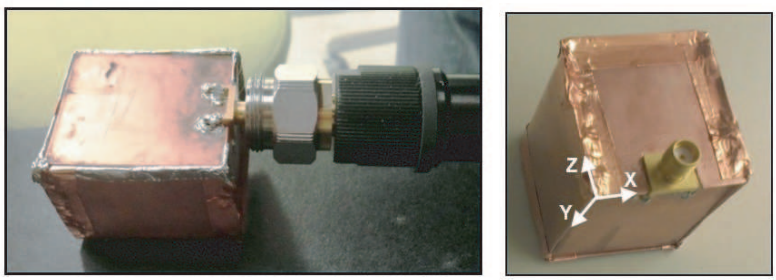

Figure 8. The rectangular Wheeler cap separately fabricated and mounted on the antenna shown in Fig. 7; cap size: XYZ: $30 \times 39 \times 30$ mm ($\sim 0.39\lambda_r \times 0.49\lambda_r \times 0.39\lambda_r$); λ_r is the wavelength at matching frequency, f_r.

5. CONCLUSION

The paper presents a methodology to miniaturize an EBG antenna using unit cells with thick metallization and narrow gaps. The effects of several modifications to the metal layer such as trimming, and interdigiting, both separately and simultaneously are demonstrated. The result is a remarkable decline in the resonance frequency while the physical size remains constant. A miniaturized unit cell occupying only 13.7% of the surface area of the basic unit cell demonstrates the potential of the approach for size reduction. Such cells were applied in the structure of a self excited EBG resonator antenna, demonstrating a drastic reduction in the matching frequency while maintaining the same physical size. A prototype SE-EBG-RA was fabricated to experimentally validate the simulations. The prototype demonstrates a high measured efficiency of more than 87%.

REFERENCES

1. Collins, S. and Y. M. M. Antar, "Antenna size reduction using Yagi-Uda loops and shorted circular patches," *IEEE Trans. Antennas Propag.*, Vol. 52, No. 3, 855–864, Mar. 2004.
2. Skrivervik, A. K., J. F. Zurcher, O. Staub, and J. R. Mosig, "PCS antenna design: The challenge of miniaturization," *IEEE Antennas Propag. Mag.*, Vol. 43, No. 4, 12–27, Aug. 2001.
3. Mosallaei, H. and K. Sarabandi, "Antenna miniaturization and bandwidth enhancement using a reactive impedance substrate," *IEEE Trans. Antennas Propag.*, Vol. 52, No. 9, 2403–2414, Sep. 2004.
4. Hosseini, M., M. Pirhadi, and M. Hakkak, "Design of a non-uniform high impedance surface for a low profile antenna," *Journal of Electromagnetic Waves and Applications*, Vol. 20, No. 11, 1455–1464, 2006.
5. Hosseini, M. and D. M. Klymyshyn, "Radiation properties of EBG textured tall transmission lines and applications: A low profile self-excited EBG resonator antenna," *IEEE Antenn. Wireless Propag. Lett.*, Vol. 11, 276–280, 2012.
6. Alphones, A. and J. Cheng, "Compact interdigitated microstrip bandpass filter with meandered EBGs," *European Microwave Conference*, 439–443, Singapore, 2009.
7. Yang, F. and Y. Rahmat-Samii, "Reflection phase characterizations of the EBG ground plane for low profile wire antenna applications," *IEEE Trans. Antennas Propag.*, Vol. 51, No. 10, 2691–2703, 2003.
8. Klymyshyn, D. M., M. Börner, D. Haluzan, E. Gono Santosa, M. Schaffer, S. Achenbach, and J. Mohr, "Vertical high-Q RF-MEMS devices for reactive lumped element circuits," *IEEE Trans. Microwave Theory Tech.*, Vol. 58, No. 11, 2976–2986, Nov. 2010.
9. Jahani, S., J. Rashed-Mohassel, and M. Shahabadi, "Miniaturization of circular patch antennas using MNG metamaterials," *IEEE Antenn. Wireless Propag. Lett.*, Vol. 9, 1194–1196, 2010.
10. Sable, N., S. Gharat, J. Bhosale, S. Khobragade, and V. R. Anitha, "Study of Koch monopole fractal antenna," *General Assembly and Scientific Symposium, URSI*, 1–4, Istanbul, Turkey, Aug. 2011.
11. Toyota, Y., K. Iokibe, R. Koga, A. E. Engin, T. H. Kim, and M. Swaminathan, "Miniaturization of electromagnetic bandgap (EBG) structures with high-permeability magnetic metal sheet," *IEEE Symp. on Electromagnetic Compatibility*, 1-5, Honolulu, Hawaii, USA, Jul. 2007.
12. Chi, P. L., R. Waterhouse, and T. Itoh, "Antenna miniaturization using slow wave enhancement factor from loaded transmission line models," *IEEE Trans. Antennas and Propag.*, Vol. 59, No. 1, 48–57, Jan. 2011.
13. Hosseini, M., A. Pirhadi, and M. Hakkak, "Compact angularly stable AMCs utilizing skewed cross-shaped FSSs," *Microw Opt. Technol. Lett.*, Vol. 49, No.4, 781–786, Apr. 2007.
14. Lamminen, A. E. I., A. R. Vimpari, and J. Saily, "UC-EBG on LTCC for 60-GHz frequency band antenna application," *IEEE Trans. Antennas Propag.*, Vol. 57 , No. 10, 2904–2912, Oct. 2009.
15. Sievenpiper, D. F., *High-impedance Electromagnetic Surfaces*, PhD thesis, Univ. Calif., LA, USA, 1999.

16. Lin, B.-Q., J. Liang, Y.-S. Zeng, and H.-M. Zhang, "A novel compact and wide-band uni-planar EBG structure," *Progress In Electromagnetics Research C*, Vol. 1, 37–43, 2008.
17. Antoniades, M. A. and G. V. Eleftheriades, "A CPS leaky-wave antenna with reduced beam squinting using NRI-TL metamaterials," *IEEE Trans. Antennas Propag.*, Vol. 56, No. 3, 708–721, Mar. 2008.
18. Coulombe, M., S. Farzaneh Koodiani, and C. Caloz, "Compact elongated mushroom (EM)-EBG structure for enhancement of patch antenna array performances," *IEEE Trans. Antennas and Propag.,* Vol. 58, No. 4, 1076–1086, Apr. 2010.
19. Hosseini, M. and D. M. Klymyshyn, "A low profile efficient leaky-wave antenna composed of high aspect ratio EBG unit cells," *IEEE Radio and Wireless Symp.*, 229–231, Austin, TX, USA, Jan. 20–23, 2013.
20. Hosseini, M. and M. Hakkak, "Characteristics estimation for Jerusalem cross based artificial magnetic conductors," *IEEE Antenn. Wireless Propag. Lett.*, Vol. 7, 58–61, 2008.
21. Merli, F., L. Bolomey, J. Zurcher, G. Corradini, E. Meurville, and A. K. Skrivervik, "Design, realization and measurements of a miniature antenna for implantable wireless communication systems," *IEEE Trans. Antennas and Propag.*, Vol. 59, No. 10, 3544–3555, Oct. 2011.
22. Pozar, D. M. and B. Kaufman, "Comparison of three methods for the measurement of printed antenna efficiency," *IEEE Trans. Antennas and Propag.*, Vol. 36, No. 1, 136–139, Jan. 1988.